2020

NiS2 as a broadband saturable absorber for ultrafast pulse lasers

Pengfei Wang

Han Zhang

Yu Yin

See next page for additional authors

Funder: National Key R&D Program of China; National Natural Science Foundation of China (NSFC); Science Foundation Ireland

Authors

Pengfei Wang, Han Zhang, Yu Yin, Qiuyun Ouyang, Yujin Chen, Elfed Lewis, Gerald Farrell, Masaki Tokurakawa, Sulaiman Wadi Harun, Cong Wang, and Shi Li

Optics and Laser Technology 132 (2020) 106492

Contents lists available at ScienceDirect

Optics and Laser Technology

journal homepage: www.elsevier.com/locate/optlastec

Full length article

NiS_2 as a broadband saturable absorber for ultrafast pulse lasers

Pengfei Wang[a,b], Han Zhang[a,c], Yu Yin[b], Qiuyun Ouyang[b], Yujin Chen[b], Elfed Lewis[d], Gerald Farrell[e], Masaki Tokurakawa[f], Sulaiman Wadi Harun[g], Cong Wang[a,c], Shi Li[b,*]

[a] Key Laboratory of Optoelectronic Devices and Systems of Ministry of Education and Guangdong Province, College of Optoelectronic Engineering, Shenzhen University, Shenzhen 518060, China
[b] Key Laboratory of In-fibre Integrated Optics of Ministry of Education, College of Physics and Optoelectronic Engineering, Harbin Engineering University, Harbin 150001, China
[c] Collaborative Innovation Centre for Optoelectronic Science & Technology, and Key Laboratory of Optoelectronic Devices and Systems of Ministry of Education, Shenzhen 518060, China
[d] Optical Fibre Sensors Research Centre, Department of Electronic and Computer Engineering, University of Limerick, Limerick, Ireland
[e] Photonics Research Centre, Technological University Dublin, Dublin, Ireland
[f] Institute for Laser Science, University of Electro-Communications, 1-5-1 Chofugaoka Chofu, Tokyo 182-8585, Japan
[g] Department of Electrical Engineering, University of Malaya, 50603 Kuala Lumpur, Malaysia

HIGHLIGHTS

- The non-linear absorption (NLA) property of the NiS_2 was investigated using an open-aperture Z-scan method.
- Picosecond pulse was generated in the Yb-doped fibre laser.
- Femtosecond pulse was generated in an Er-doped fibre laser.

ARTICLE INFO

Keywords:
NiS_2
Mode-locked fibre laser
Ultrafast pulse

ABSTRACT

Nickel disulfide (NiS_2) has recently been found to possess strong nonlinear saturable absorption properties. This feature is highly attractive for nonlinear photonics applications. Ultrafast pulse generation is successfully demonstrated in this article for both Ytterbium- and Erbium-doped fibre lasers using micro-fibre deposited nickel disulfide (NiS_2) as a saturable absorber (SA). The fabricated SA device has a modulation depth of 23% at 1.06 μm and 30.8% at 1.55 μm. Stable dissipative soliton operation was achieved at 1064.5 nm with a pulse duration of 11.7 ps and another stable conventional soliton pulse train was also obtained at 1560.2 nm with a pulse duration of 524 fs. These results demonstrate that the microfibre-based NiS_2 has a broadband nonlinear response and can function as an efficient SA, therefore it has significant potential for use in ultrafast laser pulse generation.

1. Introduction

Recently, ultrafast fiber lasers have attracted significant attention given their suitability for use in a wide range of important applications including communications [1], machining [2] and sensing [3].They are also used in fundamental scientific research to investigate nonlinear characteristics of materials [4], soliton evolution [5,6], etc. Ultrafast fiber lasers have recently experienced rapid development based on saturable absorber (SA) materials, which play a crucial role in achieving passive mode-locking operation due to their simple fabrication and excellent saturable absorption characteristics [7–15]. To date, many materials including graphene [4,16–21], black phosphorus [9,22–29], Xenes [30,31], MXene [32–35], metal–organic framework [36], topological insulators [37–41], Epsilon-near-zero medium [42] and transition metal dichalcogenides (TMDs) [10–15,43–57] have been demonstrated as SAs. These materials play a crucial role in achieving passive mode-locking operation due to their simple fabrication and excellent saturable absorption characteristics.

Among these materials, transition metal dichalcogenides (TMDs) have been preferred in photonic applications due to their superior properties such as non-zero band-gap and layer-dependent optical nonlinearities. WS_2 and MoS_2 are typical TMDs and are the two most investigated TMD materials encompassing a wide range of applications including optical modulation [58], photodetectors [59], and especially

* Corresponding author.
E-mail address: m18204313488@163.com (S. Li).

https://doi.org/10.1016/j.optlastec.2020.106492
Received 5 February 2020; Received in revised form 12 July 2020; Accepted 14 July 2020
Available online 27 July 2020
0030-3992/

passively Q-switched and mode-locked lasers [11,13]. Recently, more TMDs have also been investigated in the fields of ultrafast optics. For instance, *Wang et al.* obtained 1.25 ps pulse operation with 2.13 nJ pulse energy by employing microfibre-based WTe_2 in a thulium-doped fibre laser [14]. Using SnS_2-PVA film as an SA, a femtosecond soliton pulse at 1.55 μm was reported by *Niu et al.* [15]. Research on the applications of TMDs to achieve mode-locked pulse operation continues to progress and thus it is of great interest to explore new TMDs for ultrafast fibre laser applications.

Nickel disulfide (NiS_2), another new type of TMD, has also attracted significant attention in recent years owing to its superior electrical [60,61] and optoelectronic properties [62]. NiS_2 is a semiconductor, similar to WS_2 and MoS_2 [7]. Many TMDs normally have a typically large bandgap (above 1 eV), e.g. the direct bandgap of monolayer MoS_2 is about 1.8 eV and the indirect gap of the bulk material is in the range of 0.86–1.29 eV [63]. However, the bandgap of few layer NiS_2 is about 0.3 eV [64], which forms the basis for its potential application at long wavelengths (beyond 3 μm). *Li et al.* achieved Q-switched pulse operation at 1.55 and 1.9 μm using an NiS_2-PVA film in 2019 [65], which provided strong evidence for the nonlinearity and saturable absorption of NiS_2. However, there remains a lack of research on applying NiS_2 as a material in mode-locked fiber lasers to generate ultrafast pulses.

In this paper, a micro-fiber-based NiS_2 was successfully fabricated and used as a SA to generate passive mode-locked pulses in both an Ytterbium-doped fibre laser (YDFL) cavity and an Erbium-doped fiber laser (EDFL) cavity. The NiS_2-based SA has excellent saturable absorption characteristics with a modulation depth of 23% at 1064 nm and 30.8% at 1550 nm. The dissipative soliton pulse generated at 1064 nm has a pulse duration of 11.7 ps with a pulse energy of 0.84 nJ. A conventional soliton pulse was also generated centred at the wavelength of 1560.2 nm, with a pulse duration of 524 fs and pulse energy of 1.86 nJ. The experimental results described in this article clearly indicate that NiS_2 has excellent potential for use in ultrafast mode-locked fiber laser applications.

2. Characteristics of NiS_2 and experimental setup

The NiS_2 nanosheets (provided by XFNANO, XF-137Ni, 3–6 layer) were prepared using a liquid-phase exfoliation method and then dispersed in an ethanol solution with a concentration of 0.1 mg/ml for further usage. The process of preparation is explained as follows: Firstly, the NiS_2 powders were dispersed in deionized water and treated for 12-h using an ultrasonic cleaner. Then, the NiS_2 suspension was centrifuged at a rate of 5000 rpm for 15 min to remove unwanted large agglomeration. The upper supernatant was extracted as an NiS_2 solution for use in the experiment. An NiS_2 dispersion solution was prepared by adding 10 g of NiS_2 nanosheets into 100 mL alcohol (30%). After that, the mixture was placed in the ultrasonic cleaner for 12 h and centrifuged at a rate of 2000 rpm for 30 min for further use.

It was necessary to characterize structure of NiS_2 before using in the mode-locked fiber laser. A scanning electron microscopy (SEM) image of the NiS_2 nanosheets is shown in Fig. 1(a). Fig. 1(b) shows the transmission electron microscopy (TEM) image of the same NiS_2 nanosheets. Both SEM and TEM results show that NiS_2 has a typical layered structure. In order to further confirm the elementary composition of the NiS_2 nanosheets, the Raman spectrum was measured and is shown in Fig. 1(c). Two weak peaks were observed at 274.0 cm^{-1} and 284.8 cm^{-1} which correspond to the S-S pair vibrational modes (T_g and E_g). The two strong peaks at 479.7 cm^{-1} and 489.8 cm^{-1} correspond to stretching modes of the S-S pair (A_g and T_g). The Raman spectrum result confirmed the existence of NiS_2 and the result agrees well with earlier findings [66]. Furthermore, the linear transmission curve of the NiS_2 nanosheets sample (NiS_2 nanosheets dispersed in ethanol solution) was measured and recorded in Fig. 1(d) within the range of 1000 nm to confirm the material's suitability for use as a SA. For reference the transmission was measured as 78.8% at 1064 nm and 80.5% at 1560.2 nm, the operating wavelengths of the YDFL and EDFL respectively as measured using a UV/Vis/NIR spectrophotometer (Perkin-Elmer Lambda 750).

To enhance the reliability of the NiS_2 SA, the NiS_2 nanosheets were deposited directly on the waist region of the microfibre [8,67]. A microfibre-based SA structure is attractive as a way to increase the power tolerance of the device by making use of the microfibre's strong evanescent field effect. This is beneficial in the goal of obtaining higher output power [43]. In this work, the microfibre waist region was coated with the NiS_2 nanosheets. The fabricated microfibre-based material is more effective in avoiding thermal effects [22]. The use of a longer waist region also allows greater light matter interaction to occur via the evanescent field and the NiS_2 material as well as providing the required strong nonlinear optical response to facilitate pulse generation [22].

The preparation process of the microfibre-based NiS_2 involves a series of steps as follows. The microfibre was fabricated by heating and stretching a standard single-mode fibre (SMF-28) using the fused taper method [8]. The fabricated microfibre has a waist diameter of ~4.5 μm and effective tapered region of ~1.5 cm length. Source light (50 mW) provided from a 980 nm laser (MCPL-SM-980) was launched into the microfibre, which was immersed in the NiS_2 solution for more than 3 h to deposit the NiS_2 nanosheets onto the surface of the microfibre waist. Fig. 1(e) and (f) show the optical microscope images of the waist region of a microfibre sample without and with the deposited NiS_2 nanosheets respectively. Compared with the smooth surface of the microfiber in Fig. 1(e), it is clear that there are sediments on the surface of the microfiber in Fig. 1(f), which indicated that the NiS_2 nanosheets were successfully deposited onto the surface of the microfiber.

The non-linear absorption (NLA) property of the NiS_2 (NiS_2 nanosheets dispersion in ethanol solution) was investigated using an open-aperture Z-scan method [39]. The experimental setup is shown in Fig. 2(a). Three excitation sources with wavelengths centred at 800 nm (from a Ti: sapphire laser system, pulse duration: 200 fs, repetition rate: 2 kHz), 1064 nm (in-house developed source, pulse duration: 50 ps, repetition rate: 1 kHz) and 1550 nm (in-house developed source, pulse duration: 50 ps, repetition rate: 1 kHz) were applied to perform the characterizations. The laser source imposed a limitation that meant it had to be used with different parameters at a different wavelength. Thus, the pump power was optimized to ensure that the pulse energy remained constant, which is necessary to observe whether the NiS_2 exhibits similar nonlinearity at different wavelengths. Typical NLA behavior was observed at 800 nm, 1064 nm and 1550 nm, as depicted in Fig. 2(b)–(d), which exhibited typical SA characteristics. According to the results shown in Fig. 2(b)–(d), as the input power increases, all the normalized transmittances gradually increase with a decrease in the distance between the sample and the focus point ($Z = 0$) at 800 nm, 1064 nm and 1550 nm, which are caused by the well-established optical saturable absorption effect [65]. In addition, the normalized z-scan transmissions show typical nonlinear transmission characteristics under different excitation pulse energies at different wavelengths. The open-aperture Z-scan curves in Fig. 2 were fitted by using the following equations [15]:

$$T(z) = \left[1 - \frac{\alpha_0 L I_s}{I_s + I_0/(1 + z_2/z_0^2)}\right]/(1 - \alpha_0 L) \quad (1)$$

$$T(z) = 1 - \frac{\beta I_0 L_{eff}}{2\sqrt{2}(1 + z_2/z_0^2)} \quad (2)$$

$$L_{eff} = \left(1 - e^{-\alpha_0 L}\right)/\alpha_0 \quad (3)$$

where z is the sample position relative to the focus position, z_0 is the diffraction length of the beam, $\alpha_0 L$ is the modulation depth, $T(z)$ is the normalized transmittance at z, I_0 is peak on-axis intensity at focus, and I_s is the saturable intensity. The values of nonlinear absorption coefficient β were obtained at 800 nm, 1064 nm and 1550 nm are −98.1 cm/

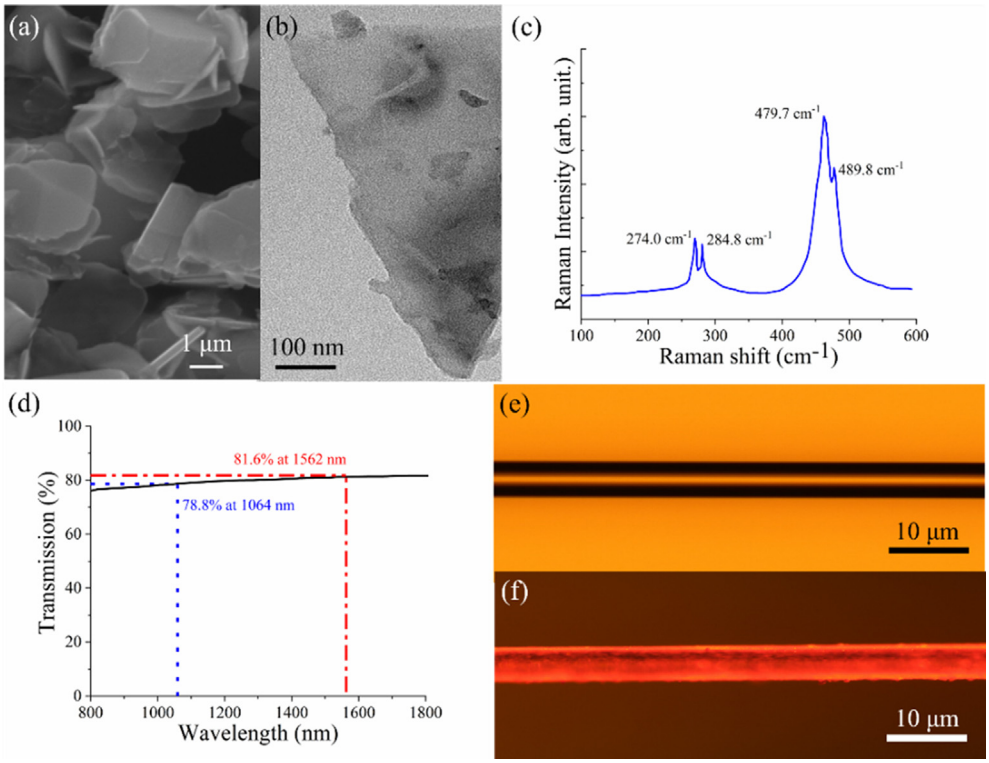

Fig. 1. (a) SEM Image of the NiS_2 sample. (b) TEM image of the NiS_2 sample. (c) Raman spectrum of the NiS_2 sample. (d) Linear transmission of the NiS_2 sample. Optical microscope images of the waist region of the microfibre (e) without and (f) with the deposited NiS_2.

GW, −65.4 cm/GW and −38.8 cm/GW. All the results indicate that NiS_2 exhibits a broadband optical nonlinear response. The absence of any clear response for a blank quartz slide under the same and even higher excitation intensity is noteworthy, which suggests the significant SA response arises from the nonlinear modulation effect of NiS_2. This indicates that low intensity light is effectively suppressed but higher intensity light can be output with little or no attenuation. That is to say, the NiS_2 can serve as an ultrafast nonlinear saturable absorber, as well as a passive mode-locking modulator for ultrashort pulsed lasers generation in the near-infrared region.

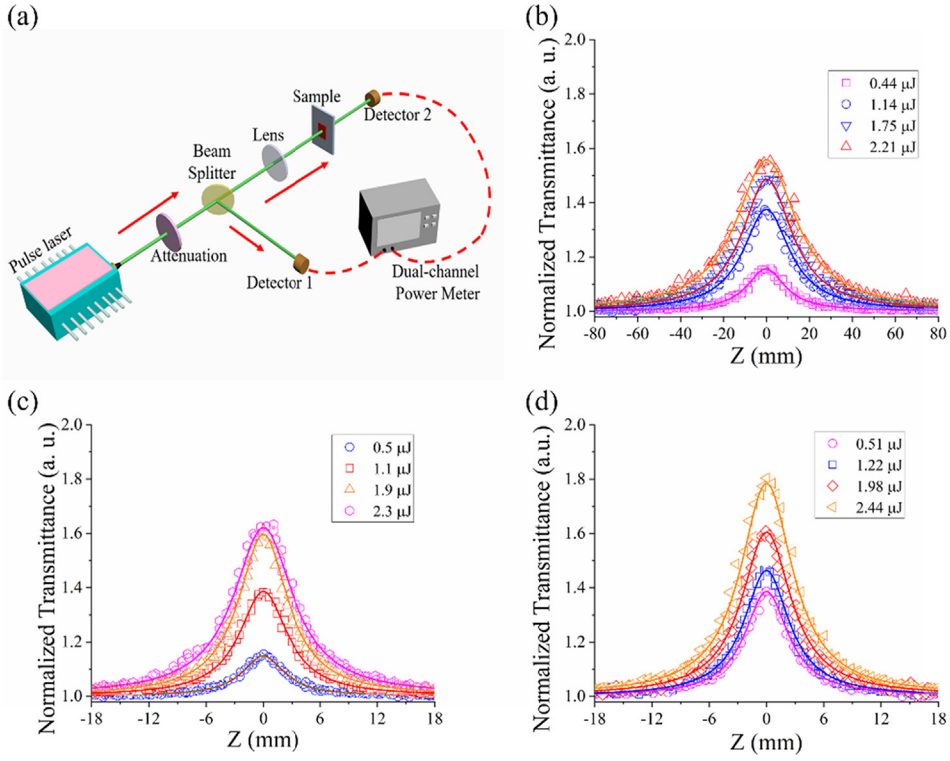

Fig. 2. (a) Experimental setup of the Z-scan testing platform. The typical Z-scan peak curve of NiS_2 at 800 nm (b), 1064 nm (c), 1550 nm (d).

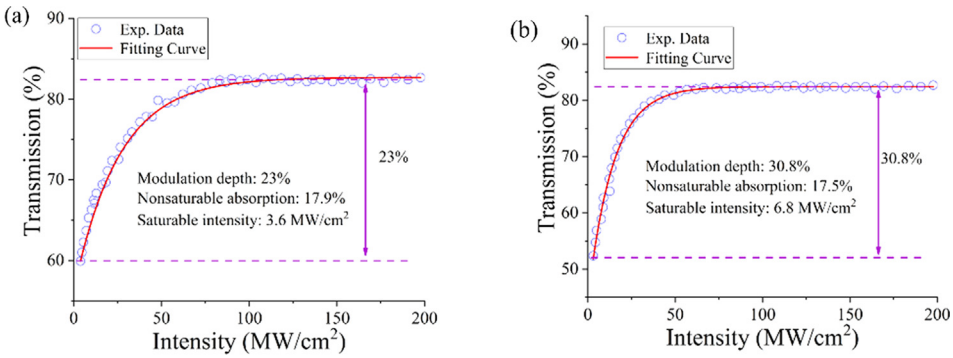

Fig. 3. (a) The nonlinear absorption of microfibre-based NiS_2 at 1.06 μm. (b) The nonlinear absorption of microfibre-based NiS_2 at 1.55 μm.

In addition, the nonlinear transmission characteristic of the NiS_2 was also investigated at the wavelengths of 1.06 μm and 1.55 μm as shown in Fig. 3(a) and (b) using a twin-balanced measurement. The blue circles represent the experimental data, which confirms a trend consistent with nonlinear absorption. The red solid curve represents the fitted line of the experimental data based on a simplified two-level saturable absorption model [68], which clearly indicates the presence of a typical saturable absorption effect. The saturable absorption modulation depth, the non-saturable absorption and the saturable intensity were determined as 23%, 17.9% and 3.6 MW/cm^2 respectively at the wavelength of 1.06 μm, which are shown in Fig. 3(a). For the case of 1.55 μm, the three corresponding values are 30.8%, 17.5% and 6.8 MW/cm^2, as shown in Fig. 3(b). The anisotropic features normally influence the polarization-induced absorption such as ReS_2 [69]. In fact, for any polarization direction the ReS_2-D shaped fiber SA exhibits saturable absorption with a similar modulation depth. NiS_2 should therefore exhibit similar behavior as it is a semiconductor and similar to ReS_2. The polarization induced absorption in the microfiber is smaller than in the case of the D-shape fiber.

Fig. 4 shows the configuration of the fibre laser used in this investigation, which includes the fabricated microfibre-based NiS_2 as the SA device. The pump source provides 976 nm photons to pump the gain medium. It was optically coupled into a section of gain medium via a wavelength division multiplexer (WDM). The power generated in the gain medium propagates into the polarization independent isolator (PI-ISO), which was connected to an 80:20 optical coupler (OC) to provide a monitor output. The SA device was spliced between the 80%-output port of the OC and the WDM to complete the ring cavity. The 20% output port of the OC was connected to an optical spectrum analyzer

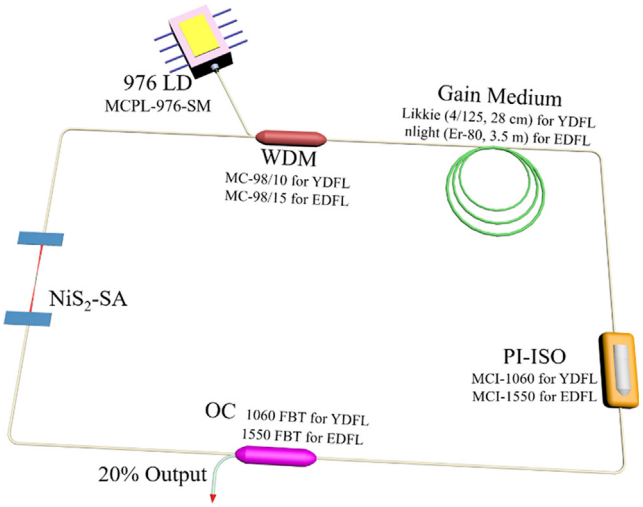

Fig. 4. Schematic diagram of the passively mode-locked fibre laser operated at 1.06 and 1.55 μm.

(OSA, YOKOGAWA, AQ-6370B) to measure the output spectrum of the laser. The time resolved output signal of the pulsed laser was also measured using a digital storage Oscilloscope (Tektronix MDO4054-6, 6 GHz) and a photodetector (Kemai, PDA, 10 GHz). A radio frequency (RF) spectrum analyzer (Anritsu, MS2683A) was employed to record the RF spectrum of the mode-locking operation. In addition, the pulse duration was measured using a commercial auto-correlator instrument (APE Pulsecheck). An optical power meter (Newport 1918-R) was used to measure the light output power.

3. Results and discussion

3.1. Picosecond pulse generation in the YDFL

For the YDFL case, a 28 cm section of Yb-doped fibre (YDF, Liekki, 4/125) with a dispersion parameter of −43 ps/(nm·km) at 1060 nm was used as the gain medium. The total cavity length of the YDFL was about 4.98 m providing a net dispersion of 0.114 ps^2. A continuous wave (CW) laser was used as the pump source which was able to achieve a pump power of 65 mW. Mode-locked operation occurred when the pump power was increased to 89 mW. Stable mode-locking could be obtained when the pump power was varied from 89 mW to the maximum of 700 mW. The maximum output power was measured to be 35.6 mW when the pump power was set to the maximum available value of 700 mW, corresponding to a pulse energy of 0.84 nJ. The relationship between the pump power and the output power is shown in Fig. 5(a). Fig. 5(a) also shows that the output power exhibited an excellent linear relationship with the pump power, having a slope efficiency of 5.1% up to the maximum pump value of 700 mW. A linear regression analysis of the data of output power versus pump power yielded a linear coefficient (R^2) value of 0.997. The characteristics of the soliton pulse at the pump power of 700 mW are also summarized in Fig. 5. Fig. 5(b) shows the typical soliton spectrum of the pulse centred at 1064.5 nm. The observed 3-dB spectral bandwidth is 7.8 nm. The spectrum with step edges exhibit characteristics which are typical of dissipative soliton operation in the all-normal dispersion region [70]. Fig. 5(c) shows the corresponding oscilloscope trace with a pulse train of period 23.6 ns. The autocorrelation trace of the mode-locked pulses has an 18-ps full width at half maximum (FWHM) and this is shown in Fig. 5(d). The real pulse duration is 11.7 ps when a Gaussian fitting is assumed. The time-bandwidth product (TBP) was calculated to be 24.16, which indicated that the pulse operation was strongly chirped. The pulse duration is much larger than that of common dissipative soliton lasers for such a short cavity length. This was due to the relatively narrow spectrum of 7.8 nm and due to the existence of the filter effect, corresponding to a Gaussian Fourier-transform-limited pulse width of 213.6 fs. Furthermore, the all-normal dispersion cavity had a large net positive dispersion, which also contributed to the large pulse width. With suitable extra-cavity compression by dispersion-compensation elements, the pulse width could be compressed to less than 1 ps

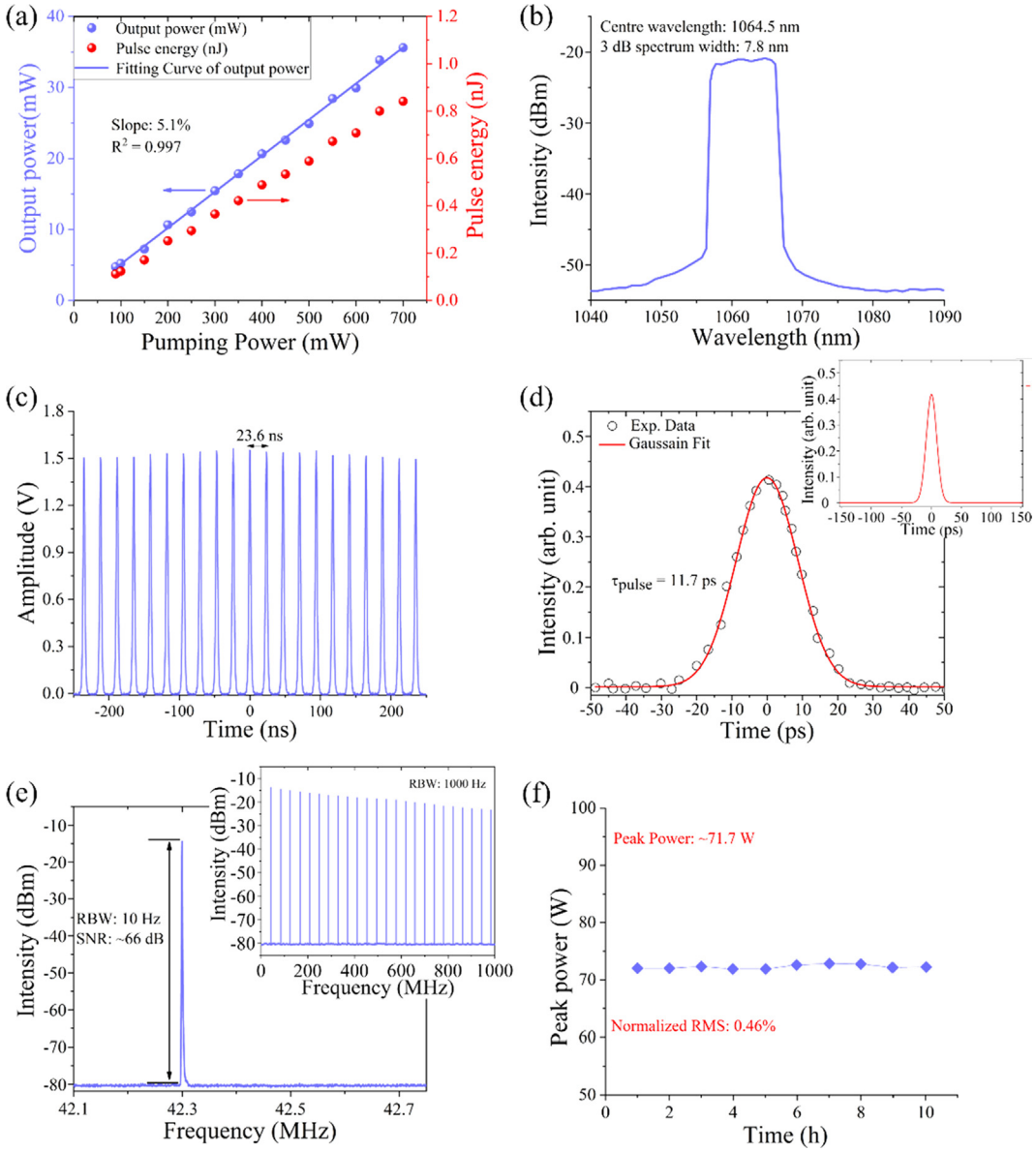

Fig. 5. Characteristics of the picosecond pulse in YDFL. (a) Relationship between the pump power and laser output power. (b) The Measured 0ptical spectrum with a bandwidth of 7.8 nm. (c) Typical oscilloscope pulse waveform. (d) Autocorrelation trace for an output pulse with a pulse duration of 11.7 ps. The inset is the autocorrelation trace of a 300-ps span. (e) RF spectrum at a fundamental frequency of 42.3 MHz with a 10 Hz resolution. The inset is the RF spectrum of a 1000 MHz span. (f) The fluctuation of peak power during a 10 h period.

[70]. The inset of Fig. 5(d) shows the autocorrelation trace with a 300-ps span, which confirms that the pulse operation at 1064.5 nm is a single soliton, and not multi-pulse operation even at the maximum pump power of 700 mW.

The stability of the pulse operation and the long-term laser output power stability performance are two important factors in fibre laser systems. The radio frequency (RF) spectrum and long-term stability (peak power fluctuation of the output spectrum during a 10 h observation period) were measured and are shown in Fig. 5(e) and (f), respectively. Fig. 5(e) presents the RF spectrum with a 10 Hz spectral resolution. The fundamental repetition rate of 42.3 MHz is consistent with the cavity roundtrip time of 23.6 ns. The signal-to-noise ratio (SNR) of the fundamental frequency obtained from Fig. 5(e) was 66 dB. The inset of Fig. 5(e) shows a substantially flat RF spectrum for a 1000 MHz span, which confirms the stability of the mode-locking operation. As shown in Fig. 5(f), the fluctuation of the highest peak power (71.7 W) of the NiS_2-based YDFL is extremely small and exhibits a high degree of invariance with time, corresponding to a normalized RMS value of 0.46%, which confirms the fibre laser has excellent long-term stability.

Normally, the YDFL has a strongly chirped pulse laser output due to the presence of a large normal dispersion, which results in a narrow 3 dB spectral width and hence a large pulse width [71,72]. However, by optimizing the SA device and the laser cavity design, the 3 dB spectral width could be increased and the pulse width therefore decreased. Increasing the small signal absorption, and reducing the saturation power of the SA enhances the output pulse parameters. More specifically, it increases the pulse energy and spectral bandwidth and decreases the temporal pulse width [73]. In the experiment of this investigation, The NiS_2-SA has a relatively large modulation depth and low saturable intensity. Due to the high optical nonlinearity of NiS_2-SA, it can be considered equivalent to a bandpass filter, which offers benefits of improved pulse shape and widened spectra. The laser cavity also has a small normal dispersion value of 0.114 ps^2 which has been achieved by optimizing the laser cavity length (laser cavity length is only 4.98 m), which also effectively decreases pulse chirp.

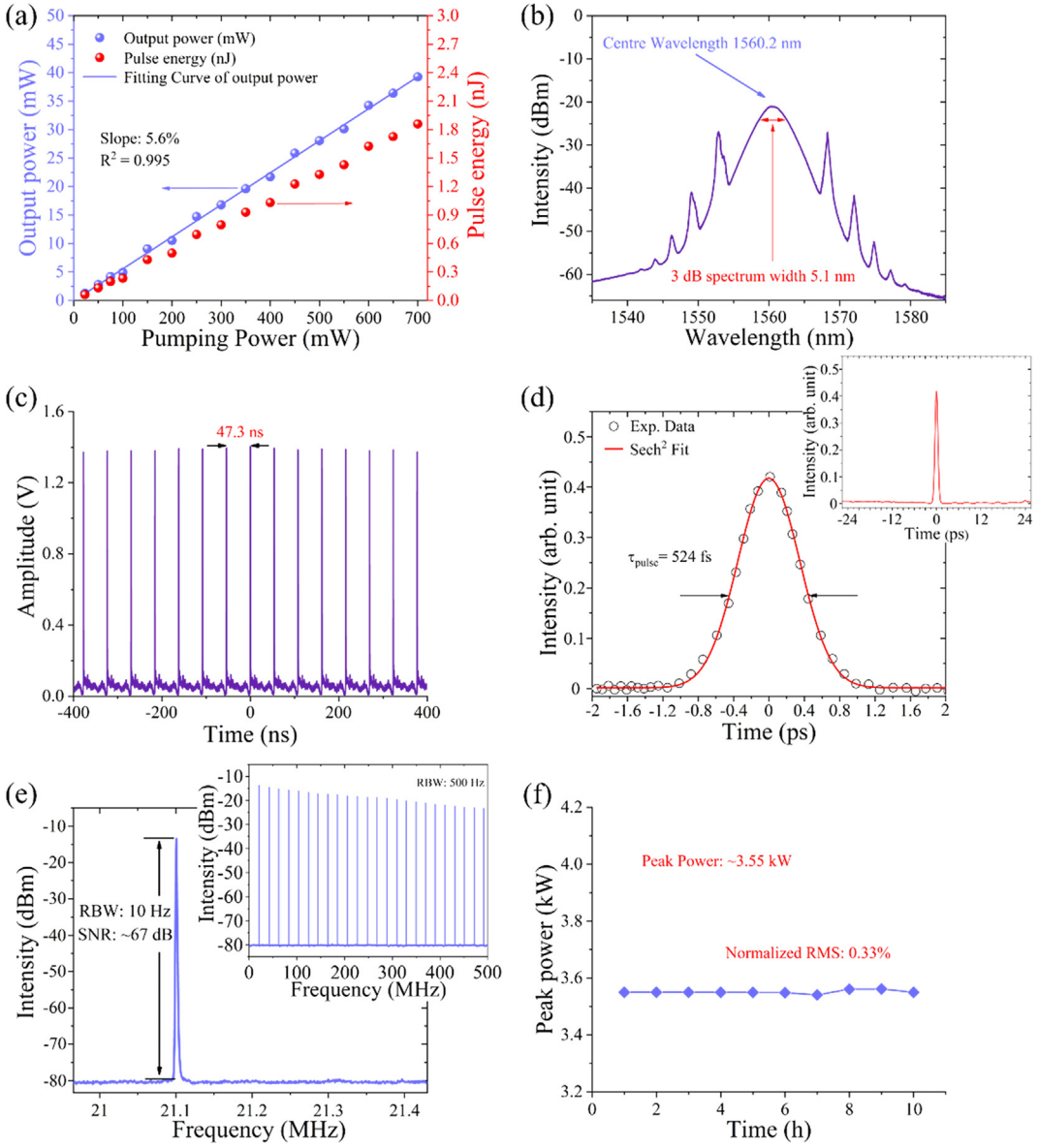

Fig. 6. Characteristics of the femtosecond pulse in the EDFL. (a) The relationship between the pump power and laser output power. (b) The measured optical spectrum with a bandwidth of 5.1 nm. (c) A typical oscilloscope pulse waveform. (d) The autocorrelation trace for an output pulse with a pulse duration of 524 fs. The inset is the autocorrelation trace of a 24 ps span. (e) RF spectrum at fundamental frequency of 21.1 MHz with a 10 Hz resolution. The inset is the RF spectrum of a 500 MHz span. (f) The fluctuation of peak power during a 10 h period.

3.2. Femtosecond pulse generation in an EDFL

In the case of the EDFL, a 3.5 m length of Er-doped fibre (EDF, nLight, Er80-8/125) with a dispersion parameter value of −16 ps/(nm·km) at 1550 nm was used as the gain medium. The total cavity length of the EDFL was about 9.8 m with a net dispersion of −0.049 ps^2. CW laser output was achieved with a pump power of 24 mW. Mode-locked operation was observed when the pump power was increased above 37 mW. The maximum output power was measured to be 39.2 mW when the pump power was set to the maximum available value of 700 mW, corresponding to a pulse energy of 1.86 nJ. The relationship between the pump power and the output power is shown in Fig. 6(a). Fig. 6(a) which also shows that the output power exhibited an excellent linear relationship with the pump power having a slope value of 5.6% up to the maximum pump value of 700 mW. A linear regression analysis of the data of output power versus pump power yielded a linear coefficient (R^2) value of 0.995. The characteristics of the soliton pulse at the pump power of 700 mW are also summarized in Fig. 6. Fig. 6(b) shows the typical soliton spectrum of the pulses, which are centred at 1560.2 nm with a 3-dB spectral bandwidth of 5.1 nm. The spectrum has a typical soliton-like shape with the characteristic Kelly sideband. Fig. 6(c) shows the time resolved (oscilloscope) waveform of the output pulse train, indicating the low peak-to-peak fluctuations and the high stability of the mode-locked pulse operation. The autocorrelation trace of the mode-locked pulses has an 810-fs full width at half maximum (FWHM) and this is shown in Fig. 6(d). The pulse duration was determined as 524 fs with a $sech^2$ fitting assumed. The time-bandwidth product (TBP) was calculated to be 0.329, which is very close to the transform-limited value (0.315). The inset of Fig. 6(d) shows the autocorrelation trace with a 24-ps span, which confirms that the femtosecond pulse is a single soliton, and not multi-pulse operation, even at the maximum pump power of 700 mW.

The pulse stability and long-term output power stability of the laser were measured using the radio frequency (RF) spectrum and a temporal long-term stability (peak power fluctuation of the output spectrum during a 10 h observation period) and are shown in Fig. 6(e) and (f),

respectively. Fig. 6(e) presents the RF spectrum with a 10 Hz spectral resolution. The fundamental repetition rate was observed as 21.1 MHz, which is consistent with the cavity roundtrip time of 47.3 ns. The signal-to-noise ratio (SNR) of the fundamental frequency obtained from Fig. 6(e) is 67 dB. The inset of Fig. 6(e) shows the RF spectrum of 500 MHz span with a resolution of 500 Hz. As shown in Fig. 6(f), the fluctuation of the highest peak power (3.55 kW) of the NiS_2-based EDFL is extremely small and exhibits a high degree of invariance with time, showing a normalized RMS of 0.33%, which confirms the fibre laser has excellent long-term stability.

3.3. Analysis

Generally, the threshold for mode-locking operation is primarily determined by the cavity loss. Typical setups involve the use of a polarization controller (PC), but this increases the cavity loss as a result of fibre bending within the PC. For the laser cavity used in this investigation, no PC was used, which avoids the large losses that would otherwise result. Losses can also be attributed to the other optical components in the laser ring including the WDM, OC and PI-ISO, in particular where the operating wavelength lies outside the low loss transmission window of such components. The wavelength deviations between the customized wavelength of the optical devices (such as the WDM and PI-ISO) and the centre wavelength of the laser can also cause significant losses. However, in this investigation the mode-locked pulse operating wavelength lies sufficiently close to the low loss transmission window of the optical devices being circa 1060 nm (YDFL case) and 1550 nm (EDFL case), again resulting in low losses within the laser cavity. The low cavity loss means that mode-locking operation in the YDFL and EDFL described in this article has a low threshold for the onset of mode-locked operation. The absence of the PC in the cavity also ensured that no nonlinear polarization evolution (NPE) effect occurred, which can potentially limit the output pulse energy [74].

According to standard soliton theorem, the pulse energy should be no more than 0.1 nJ and the pulse energy of dispersion-manage soliton is generally less than 1 nJ. However, previous reports have confirmed that more than 1 nJ pulse energy could be obtained in soliton-like pulse with typical values being 5.05 nJ [48], 2.13 nJ [14]. These results confirm that the high pulse energy reported in this article is not a unique phenomenon. In order to explain this phenomenon, some discussion is provided as follow: the transmission of pulses in fiber lasers is described by the generalized non-linear Schrodinger (NLS) equation [75]:

$$\frac{\partial A}{\partial z} + \frac{i}{2}(\beta_2 + ig_0 T_2^2)\frac{\partial^2 A}{\partial T^2} = i\left(\gamma + \frac{i}{2}\alpha_2\right)|A|^2 A + \frac{1}{2}(g_0 - \alpha)A \tag{4}$$

Eq. (4) is the generalized NLS equation of complex the coefficient, also known as the Ginzburg-Landau equation, which provides the theoretical model for the fiber laser. Soliton pulses also obey the Ginzburg-Landau equation. When the optical solitons travel thorough a fiber in a stable transmission state, the optical intensity can be described as [75]:

$$|E|^2 = k_0^{(2)} \int_0^\infty \int_0^\infty \left[\frac{\partial^2 \Delta\omega}{\partial t'^2}\Delta\omega + \left(\frac{\partial \Delta\omega}{\partial t'}\right)^2\right]\frac{1}{2\pi n_2} dt' dt \tag{5}$$

Solitons can normally be characterized using a hyperbolic secant shaped pulse, $a = sech(s)$. Due to the high average output power and high peak power in the fiber laser of this investigation, the pulse has an uncertain amplitude and shape, and this would normally result in the soliton pulse splitting. However, due to the nonlinearity and the pulse shaping ability of the 2D materials, pulse splitting and collapse are suppressed. This phenomenon is explained by the fact that an input pulse with an incorrect amplitude and shape can evolve to change exactly to the required form after passing through a short length of fiber, and thus the pulse eventually into a strict soliton [75]. Actually, the formation of high energy pulses is complicated by the presence of saturable absorbers. However, several benefits accrue from the highly nonlinear properties of NiS_2 and this, coupled with good fiber laser cavity design of the significant influence in the successful formation of high energy pules: (1) In this article, passive mode-locked operation was only possible because of the presence of the microfibre-based NiS_2 SA device. The microfibre device promotes access to the evanescent wave field and thus avoids direct transmittance of light through the SA material. This increases the high power tolerance of the device and effectively prevents dispersion caused by the SA material [43]. (2) The prepared SA when completely coated with NiS_2 nano-sheets has a modulation depth as high as 23% at a wavelength of 1060 nm and 30.8% at a wavelength of 1550 nm, and both values are well suited for generation of high energy pulses. The 0.84 nJ (YDFL case in Fig. 5 (a)) and 1.86 nJ (EDFL case in Fig. 6 (a)) for maximum output pulse energy are consistent with the presence of excellent non-linearity and an absence of NPE. (3) In the case of EDFL, it is worth noting that the spectrum of an output pulse was measured in the range 800 to 1700 nm and no signal was observed at 976 nm, indicating that there was no residual pump power, which is a direct consequence the efficient design of the resonator structure. (4) The NiS_2-SA device could still work at the high pump power of 700 mW, which indicates a high damage threshold. The high damage threshold of the NiS_2-SA device allows the laser to absorb high levels of pump power, which is one of the main reasons for the higher average output power capability of the devices produced in this investigation. The authors of this article believe that even higher output power values could be obtained by further improving the laser structure design (e.g. by reducing the cavity length) and optimizing the NiS_2-SA properties (e.g. reducing the thickness of NiS_2 by decreasing the deposition time).

Although WS_2 and MoS_2 have been reported to possess nonlinear absorption, NiS_2 exhibits some unique characteristics. As the few layer NiS_2 has a relatively small bandgap, it is believed that NiS_2 could be used for longer wavelength operation including mid-infrared. In contrast, WS_2 and MoS_2 have relatively large bandgap values (normally above 1 eV) when formed as a monolayer to a bulk substrate [63]. As a result, the operation wavelength and absorption intensity are clearly influenced by the bandgap: small bandgap normally means the longer wavelength absorption. The nonlinear saturable absorption of NiS_2 exhibits similar merits as discussed above. For example, the saturable intensity of few layer MoS_2 is in the range ofseveral tens of MW/cm^2, while it increases at least ten times for multilayer MoS_2. However, the bandgap of multilayer MoS_2 (smaller than the corresponding monolayer value) is better suited for longer wavelength operation including mid-infrared [63]. In the case of few layer NiS_2, the characteristics of saturable absorption are better suited for wide wavelength operation covering the range from visible to mid-infrared due to its low nonlinear absorption intensity of several MW/cm^2. In addition, the high modulation depth with a high damage threshold for ultrafast pulses have rarely been observed in the microfiber-based schemes. It is significant for the development of saturable absorber based on microfiber to show that NiS_2-SA achieves an extremely attractive modulation depth whilst exhibiting high tolerance for high pulse energy for use in ultrafast pulsed fiber lasers.

In order to better understand the high modulation depth effect of NiS_2-SA for the mode-locked fiber laser performance, the modulation depth of NiS_2-SA has been discussed in detail as follows. Modulation depth refers to the change in reflectance when the pulsed light flux is much greater than the saturation absorption flux. It characterizes the ability of the material bleached in the presence of strong pulse energy. Generally, the greater the modulation depth, the material is better suited for commencing automatic mode locking, and thus easily achieving mode locking. This has benefits for obtaining a narrow output pulse width. However, too high a modulation depth also leads to high absorption and a high non-saturation loss, which decrease the damage threshold of the SA device. On the contrary, a lower modulation depth is better for small non-saturation loss and low damage threshold.

Table 1
Comparison between the NiS_2 and other materials-based fiber lasers.

Materials	SA type	Modulation depth	Wavelength	Pulse width	Thresholds	Damage power	Ref
In_2Se_3	Sandwiched	14%	1558 nm	1.88 ps	27 mW	/	[80]
$PtSe_2$	Microfiber	4.9%	1563 nm	1.02 ps	93 mW	> 450 mW	[82]
SnSe	Microfiber	10.69%	1552 nm	960 fs	/	/	[83]
SnS_2	Sandwiched	4.6%	1562.01 nm	623 fs	125 mW	> 205 mW	[15]
NiS_2	Microfiber	30.8%	1560.2 nm	524 fs	37 mW	> 700 mW	This work

However, too low a modulation depth is not conducive to the realization of mode locking. In this experiment, the modulation depths of NiS_2-SA are 23% at1060 nm and 30.8% at 1550 nm, which are ideal for the existence of a low mode-locking threshold (37 mW for the EDFL) and narrow pulse width (524 fs for the EDFL). Additionally, the damage threshold values of YDFL and EDFL are both higher than 700 mW, which indicate that the ultra-fast pulses were realized due to the high modulation depth of NiS_2-SA and the damage threshold were not reached in each case.

The microfiber-based SA normally has a small modulation depth [76,77]. The modulation depths of the NiS_2-SA are 23% at 1064 nm and 30.8% at 1560 nm, which are consistent with results obtained in previous investigations [14]. Wang et al. prepared a WTe_2-microfiber SA using a magnetron-sputtering deposit method, which allowed accurate control of the thickness of the deposited materials [14]. The fabricated WTe_2-microfiber SA had a modulation depth of 31%. The NiS_2-SA reported in this article was prepared using a purely optical deposition method which also allowed excellent control of the layer thickness. High modulation depth values have also been reported in previous articles: 19% for graphene-microfiber [78], 16% for BP-microfiber SA [79], 14% for In_2Se_3-microfiber SA [80], 11% for graphdiyne-microfiber SA [81]. In order to obtain a higher modulation depth and lower saturable intensity for better performance of the ultrafast fiber laser, repeated experiments were conducted and the results indicate that the modulation depth and saturable intensity of NiS_2-SA can be optimized by adjusting the pump power and the deposition time. The low pump power of the source light combined with the long deposition time of the process is beneficial for creating a high modulation depth and low saturable intensity. Thus, a pump power of 50 mW and deposition time of 3 h were used during the fabrication of the NiS_2-SA reported in this article. High modulation depth (23% and 30.8% at wavelengths1064 nm and 1562 nm) and low saturable intensity (3.6 MW/cm^2 and 6.8 MW/cm^2) respectively were achieved.

It should be noted that different types of soliton have been obtained in different fibre lasers: a dissipative soliton in YDFL with positive net dispersion and a conventional soliton in EDFL with anomalous net dispersion. Under different dispersion maps, fibre lasers emit pulses with distinct characteristics, such as spectral profile, bandwidth, pulse width and repetition rate, which imply that the intracavity pulse evolution is different even though the same NiS_2 SA was used. In the case of the YDFL, the spectral profile exhibited the typical dissipative soliton characteristics of step edges [70]. The fundamental repetition rate of 42.3 MHz is consistent with the cavity roundtrip time of 23.6 ns, which confirmed the pulse operation is mode-locked. In the case of the EDFL, the conventional soliton spectrum has a typical soliton-like shape with the characteristic Kelly sideband [15]. The fundamental repetition rate is 21.1 MHz which is consistent with a cavity roundtrip time of 47.3 ns, which also confirmed the pulse operation is mode-locked. These results therefore confirm the capability of the NiS_2-based mode locker of initiating pulse operation.

In order to compare the performance of the fiber lasers based on 2D materials investigated in recent years, important parameters of these reported 2D materials-based fiber lasers (including In_2Se_3, $PtSe_2$, SnSe and SnS_2) and this NiS_2-based fiber laser are included in Table 1. It can be seen that NiS_2 is a promising alternative for low threshold, narrow pulse width and high damage power femtosecond mode-locked fiber lasers. The NiS_2-SA material benefits from a large modulation depth, small nonsaturable absorption and low saturation intensity.

In the case of both YDFL and EDFL, there still exists some uncertainty that pulse operation may be derived from the microfibre rather than NiS_2. In order to eliminate this possibility, the NiS_2 SA was replaced by the same sized microfibre, but not coated with the NiS_2 nano-sheet or any other material i.e. simply a bare fibre. When this was inserted in the laser cavity of the YDFL and EDFL, even if the pump power was adjusted gradually and carefully over a large range (to a maximum value of 700 mW), pulses were not observed. The results fully confirm that the soliton pulsed operation in the fibre lasers of this investigation is due only to the presence of the saturable absorption of the NiS_2-SA.

4. Conclusion

In conclusion, a mode-locked fibre laser (YDFL and EDFL) was successfully demonstrated by employing the microfibre-based NiS_2 SA in the laser cavity. In the YDFL case, dissipative soliton pulsed output was successfully achieved at a centre wavelength of 1064.5 nm with a 3-dB spectral bandwidth of 7.8 nm. The observed duration of the soliton pulse was 11.7 ps with signal-to-noise ratio, maximum average output power and pulse energy values of 66 dB, 35.6 mW and 0.84 nJ respectively. In the EDFL case, conventional soliton pulsed output was successfully achieved at a 1560.2 nm centre wavelength with a 3-dB spectral bandwidth of 5.1 nm. The observed duration of the soliton pulse was 524 fs with signal-to-noise ratio, maximum average output power and pulse energy values of 67 dB, 39.2 mW and 1.86 nJ, respectively. The results suggest that the microfibre-based NiS_2 SA possesses a useful broadband nonlinearity and saturable absorption. It could also be used as an excellent photonic device for ultrafast pulse generation in fibre laser applications.

Funding

National Key R&D Program of China (2016YFE0126500); National Natural Science Foundation of China (NSFC) (61575050); The fundamental research funds for the central universities (HEUCFG201841, 3072019CF2513); Key Program for Natural Science Foundation of Heilongjiang Province of China (ZD2016012, JJ2019LH0837); Open Fund of the State Key Laboratory on Integrated Optoelectronics (IOSKL2016KF03); the 111 project to the Harbin Engineering University (B13015). Professor Elfed Lewis is co-author on this publication and is supported by Science Foundation Ireland under the Centres research program (SFI/12/RC/2302_P2) for the MaREI project.

Declaration of Competing Interest

The authors declare that they have no known competing financial interests or personal relationships that could have appeared to influence the work reported in this paper.

References

[1] Z. Li, A. Heidt, J. Daniel, Y. Jung, S. Alam, D.J. Richardson, Thulium-doped fiber amplifier for optical communications at 2 μm, Opt. Express 21 (2013) 9289–9297.

[2] J. Meijer, K. Du, A. Gillner, D. Hoffmann, V. Kovalenko, T. Masuzawa, A. Ostendorf, R. Poprawe, W. Schulz, Laser machining by short and ultrashort pulses, state of the art and new opportunities in the age of the photons, CIRP Ann. 51 (2002) 531–550.

[3] F.J. McAleavey, J. O'Gorman, J.F. Donegan, B.D. MacCraith, J. Hegarty, G. Mazé, Narrow linewidth, tunable Tm/sup 3+/-doped fluoride fiber laser for optical-based hydrocarbon gas sensing, IEEE J. Sel. Top. Quantum Electron. 3 (1997) 1103–1111.

[4] Z. Sun, T. Hasan, F. Torrisi, D. Popa, G. Privitera, F. Wang, F. Bonaccorso, D.M. Basko, A.C. Ferrari, Graphene mode-locked ultrafast laser, ACS Nano 4 (2010) 803–810.

[5] P. Grelu, N. Akhmediev, Dissipative solitons for mode-locked lasers, Nat. Photonics 6 (2012) 84.

[6] Y. Song, X. Shi, C. Wu, D. Tang, H. Zhang, Recent progress of study on optical solitons in fiber lasers, Appl. Phys. Rev. 6 (2019) 021313.

[7] M. Xu, T. Liang, M. Shi, H. Chen, Graphene-like two-dimensional materials, Chem. Rev. 113 (2013) 3766–3798.

[8] S. Li, Y. Yi, Y. Yin, Y. Jiang, H. Zhao, Y. Du, Y. Chen, E. Lewis, G. Farrell, S.W. Harun, A microfiber knot incorporating a tungsten disulfide saturable absorber based multi-wavelength mode-locked erbium-doped fiber laser, J. Lightwave Technol. 36 (2018) 5633–5639.

[9] Z. Qin, G. Xie, H. Zhang, C. Zhao, P. Yuan, S. Wen, L. Qian, Black phosphorus as saturable absorber for the Q-switched Er: ZBLAN fiber laser at 2.8 μm, Opt. Express 23 (2015) 24713–24718.

[10] H. Ramakrishna Matte, A. Gomathi, A.K. Manna, D.J. Late, R. Datta, S.K. Pati, C. Rao, MoS2 and WS2 analogues of graphene, Angew. Chem. Int. Ed. 49 (2010) 4059–4062.

[11] J. Lee, J. Park, J. Koo, Y.M. Jhon, J.H. Lee, Harmonically mode-locked femtosecond fiber laser using non-uniform, WS2-particle deposited side-polished fiber, J. Opt. 18 (2016) 035502.

[12] S. Zhang, N. Dong, N. McEvoy, M. O'Brien, S. Winters, N.C. Berner, C. Yim, Y. Li, X. Zhang, Z. Chen, Direct observation of degenerate two-photon absorption and its saturation in WS2 and MoS2 monolayer and few-layer films, ACS Nano 9 (2015) 7142–7150.

[13] B. Chen, X. Zhang, K. Wu, H. Wang, J. Wang, J. Chen, Q-switched fiber laser based on transition metal dichalcogenides MoS 2, MoSe 2, WS 2, and WSe 2, Opt. Express 23 (2015) 26723–26737.

[14] J. Wang, Z. Jiang, H. Chen, J. Li, J. Yin, J. Wang, T. He, P. Yan, S. Ruan, Magnetron-sputtering deposited WTe 2 for an ultrafast thulium-doped fiber laser, Opt. Lett. 42 (2017) 5010–5013.

[15] K. Niu, R. Sun, Q. Chen, B. Man, H. Zhang, Passively mode-locked Er-doped fiber laser based on SnS 2 nanosheets as a saturable absorber, Photonics Res. 6 (2018) 72–76.

[16] V. Mamidala, R. Woodward, Y. Yang, H. Liu, K.K. Chow, Graphene-based passively mode-locked bidirectional fiber ring laser, Opt. Express 22 (2014) 4539–4546.

[17] M. Liu, R. Tang, A.-P. Luo, W.-C. Xu, Z.-C. Luo, Graphene-decorated microfiber knot as a broadband resonator for ultrahigh-repetition-rate pulse fiber lasers, Photonics Res. 6 (2018) C1–C7.

[18] Z.-R. Cai, M. Liu, S. Hu, J. Yao, A.-P. Luo, Z.-C. Luo, W.-C. Xu, Graphene-decorated microfiber photonic device for generation of rogue waves in a fiber laser, IEEE J. Sel. Top. Quantum Electron. 23 (2016) 20–25.

[19] M. Pawliszewska, T. Martynkien, A. Przewłoka, J. Sotor, Dispersion-managed Ho-doped fiber laser mode-locked with a graphene saturable absorber, Opt. Lett. 43 (2018) 38–41.

[20] Q. Bao, H. Zhang, Y. Wang, Z. Ni, Y. Yan, Z.X. Shen, K.P. Loh, D.Y. Tang, Atomic-layer graphene as a saturable absorber for ultrafast pulsed lasers, Adv. Funct. Mater. 19 (2009) 3077–3083.

[21] J. Lee, H. Chung, J. Koo, G. Woo, J.H. Lee, A 3-D printed saturable absorber for femtosecond mode-locking of a fiber laser, Opt. Mater. 89 (2019) 382–389.

[22] Z.-C. Luo, M. Liu, Z.-N. Guo, X.-F. Jiang, A.-P. Luo, C.-J. Zhao, X.-F. Yu, W.-C. Xu, H. Zhang, Microfiber-based few-layer black phosphorus saturable absorber for ultra-fast fiber laser, Opt. Express 23 (2015) 20030–20039.

[23] Y. Chen, G. Jiang, S. Chen, Z. Guo, X. Yu, C. Zhao, H. Zhang, Q. Bao, S. Wen, D. Tang, Mechanically exfoliated black phosphorus as a new saturable absorber for both Q-switching and mode-locking laser operation, Opt. Express 23 (2015) 12823–12833.

[24] J. Sotor, G. Sobon, M. Kowalczyk, W. Macherzynski, P. Paletko, K.M. Abramski, Ultrafast thulium-doped fiber laser mode locked with black phosphorus, Opt. Lett. 40 (2015) 3885–3888.

[25] D. Li, H. Jussila, L. Karvonen, G. Ye, H. Lipsanen, X. Chen, Z. Sun, Polarization and thickness dependent absorption properties of black phosphorus: new saturable absorber for ultrafast pulse generation, Sci. Rep. 5 (2015) 15899.

[26] H. Mu, S. Lin, Z. Wang, S. Xiao, P. Li, Y. Chen, H. Zhang, H. Bao, S.P. Lau, C. Pan, Black phosphorus–polymer composites for pulsed lasers, Adv. Opt. Mater. 3 (2015) 1447–1453.

[27] L. Yun, Black phosphorus saturable absorber for dual-wavelength polarization-locked vector soliton generation, Opt. Express 25 (2017) 32380–32385.

[28] K. Park, J. Lee, Y.T. Lee, W.K. Choi, J.H. Lee, Y.W. Song, Black phosphorus saturable absorber for ultrafast mode-locked pulse laser via evanescent field interaction, Ann. Phys. 527 (2015) 770–776.

[29] M. Zhang, Q. Wu, F. Zhang, L. Chen, X. Jin, Y. Hu, Z. Zheng, H. Zhang, 2D Black phosphorus saturable absorbers for ultrafast photonics, Adv. Opt. Mater. 7 (2018) 1800224.

[30] B. Guo, S.-H. Wang, Z.-X. Wu, Z.-X. Wang, D.-H. Wang, H. Huang, F. Zhang, Y.-Q. Ge, H. Zhang, Sub-200 fs soliton mode-locked fiber laser based on bismuthene saturable absorber, Opt. Express 26 (2018) 22750–22760.

[31] J. He, L. Tao, H. Zhang, B. Zhou, J. Li, Emerging 2D materials beyond graphene for ultrashort pulse generation in fiber lasers, Nanoscale 11 (2019) 2577–2593.

[32] X. Jiang, S. Liu, W. Liang, S. Luo, Z. He, Y. Ge, H. Wang, R. Cao, F. Zhang, Q. Wen, Broadband Nonlinear Photonics in Few-Layer MXene Ti3C2Tx (T = F, O, or OH) (Laser Photonics Rev. 12 (2)/2018), Laser Photonics Rev. 12 (2018) 1870013.

[33] X.-Y. Feng, B.-Y. Ding, W.-Y. Liang, F. Zhang, T.-Y. Ning, J. Liu, H. Zhang, MXene Ti3C2T x absorber for a 1.06 μm passively Q-switched ceramic laser, Laser Phys. Lett. 15 (2018) 085805.

[34] Y.I. Jhon, J. Koo, B. Anasori, M. Seo, J.H. Lee, Y. Gogotsi, Y.M. Jhon, Metallic MXene saturable absorber for femtosecond mode-locked lasers, Adv. Mater. 29 (2017) 1702496.

[35] J. Lee, J. Koo, Y.M. Jhon, J.H. Lee, A femtosecond pulse erbium fiber laser incorporating a saturable absorber based on bulk-structured Bi 2 Te 3 topological insulator, Opt. Express 22 (2014) 6165–6173.

[36] X. Jiang, L. Zhang, S. Liu, Y. Zhang, Z. He, W. Li, F. Zhang, Y. Shi, W. Lü, Y. Li, Ultrathin metal–organic framework: an emerging broadband nonlinear optical material for ultrafast photonics, Adv. Opt. Mater. 6 (2018) 1800561.

[37] X. Jiang, S. Gross, M.J. Withford, H. Zhang, D.-I. Yeom, F. Rotermund, A. Fuerbach, Low-dimensional nanomaterial saturable absorbers for ultrashort-pulsed waveguide lasers, Opt. Mater. Express 8 (2018) 3055–3071.

[38] Z.-C. Luo, M. Liu, H. Liu, X.-W. Zheng, A.-P. Luo, C.-J. Zhao, H. Zhang, S.-C. Wen, W.-C. Xu, 2 GHz passively harmonic mode-locked fiber laser by a microfiber-based topological insulator saturable absorber, Opt. Lett. 38 (2013) 5212–5215.

[39] C. Zhao, H. Zhang, X. Qi, Y. Chen, Z. Wang, S. Wen, D. Tang, Ultra-short pulse generation by a topological insulator based saturable absorber, Appl. Phys. Lett. 101 (2012) 211106.

[40] C. Zhao, Y. Zou, Y. Chen, Z. Wang, S. Lu, H. Zhang, S. Wen, D. Tang, Wavelength-tunable picosecond soliton fiber laser with topological insulator: Bi 2 Se 3 as a mode locker, Opt. Express 20 (2012) 27888–27895.

[41] K. Yin, B. Zhang, L. Li, T. Jiang, X. Zhou, J. Hou, Soliton mode-locked fiber laser based on topological insulator Bi 2 Te 3 nanosheets at 2 μm, Photonics Res. 3 (2015) 72–76.

[42] X. Jiang, H. Lu, Q. Li, H. Zhou, S. Zhang, H. Zhang, Epsilon-near-zero medium for optical switches in a monolithic waveguide chip at 1.9 μm, Nanophotonics 7 (2018) 1835–1843.

[43] W. Liu, L. Pang, H. Han, K. Bi, M. Lei, Z. Wei, Tungsten disulphide for ultrashort pulse generation in all-fiber lasers, Nanoscale 9 (2017) 5806–5811.

[44] S. Li, Y. Yin, G. Ran, Q. Ouyang, Y. Chen, M. Tokurakawa, E. Lewis, S.W. Harun, P. Wang, Dual-wavelength mode-locked erbium-doped fiber laser based on tin disulfide thin film as saturable absorber, J. Appl. Phys. 125 (2019) 243104.

[45] J. Lee, K. Lee, S. Kwon, B. Shin, J.H. Lee, Investigation of nonlinear optical properties of rhenium diselenide and its application as a femtosecond mode-locker, Photonics Res. 7 (2019) 984–993.

[46] R. Lü, Y. Wang, J. Wang, W. Ren, L. Li, S. Liu, Z. Chen, Y. Li, H. Wang, F. Fu, Soliton and bound-state soliton mode-locked fiber laser based on a MoS 2/fluorine mica Langmuir-Blodgett film saturable absorber, Photonics Res. 7 (2019) 431–436.

[47] Y. Jiang, L. Miao, G. Jiang, Y. Chen, X. Qi, X.-F. Jiang, H. Zhang, S. Wen, Broadband and enhanced nonlinear optical response of MoS 2/graphene nanocomposites for ultrafast photonics applications, Sci. Rep. 5 (2015) 16372.

[48] Y. Ge, Z. Zhu, Y. Xu, Y. Chen, S. Chen, Z. Liang, Y. Song, Y. Zou, H. Zeng, S. Xu, Broadband Nonlinear Photoresponse of 2D TiS2 for Ultrashort Pulse Generation and All-Optical Thresholding Devices, Adv. Opt. Mater. 6 (2018) 1701166.

[49] D. Mao, X. Cui, X. Gan, M. Li, W. Zhang, H. Lu, J. Zhao, Passively Q-switched and mode-locked fiber laser based on an ReS2 saturable absorber, IEEE J. Sel. Top. Quantum Electron. 24 (2017) 1–6.

[50] H. Xia, H. Li, C. Lan, C. Li, X. Zhang, S. Zhang, Y. Liu, Ultrafast erbium-doped fiber laser mode-locked by a CVD-grown molybdenum disulfide (MoS 2) saturable absorber, Opt. Express 22 (2014) 17341–17348.

[51] Z.-C. Luo, M. Liu, A.-P. Luo, W.-C. Xu, Two-dimensional materials-decorated microfiber devices for pulse generation and shaping in fiber lasers, Chin. Phys. B 27 (2018) 094215.

[52] H. Nie, X. Sun, B. Zhang, B. Yan, G. Li, Y. Wang, J. Liu, B. Shi, S. Liu, J. He, Few-layer TiSe 2 as a saturable absorber for nanosecond pulse generation in 2.95 μm bulk laser, Opt. Lett. 43 (2018) 3349–3352.

[53] W. Liu, M. Liu, M. Lei, S. Fang, Z. Wei, Titanium selenide saturable absorber mirror for passive Q-switched Er-doped fiber laser, IEEE J. Sel. Top. Quantum Electron. 24 (2017) 1–5.

[54] J. Koo, Y.I. Jhon, J. Park, J. Lee, Y.M. Jhon, J.H. Lee, Near-Infrared Saturable Absorption of Defective Bulk-Structured WTe2 for Femtosecond Laser Mode-Locking, Adv. Funct. Mater. 26 (2016) 7454–7461.

[55] Y.I. Jhon, J. Lee, M. Seo, J.H. Lee, Y.M. Jhon, van der Waals Layered Tin Selenide as Highly Nonlinear Ultrafast Saturable Absorber, Adv. Opt. Mater. 7 (2019) 1801745.

[56] X. Tian, R. Wei, M. Liu, C. Zhu, Z. Luo, F. Wang, J. Qiu, Ultrafast saturable absorption in TiS 2 induced by non-equilibrium electrons and the generation of a femtosecond mode-locked laser, Nanoscale 10 (2018) 9608–9615.

[57] Y. Ge, Z. Zhu, Y. Xu, Y. Chen, S. Chen, Z. Liang, Y. Song, Y. Zou, H. Zeng, S. Xu, H. Zhang, D. Fan, Broadband nonlinear photoresponse of 2D TiS_2 for ultrashort pulse generation and all-optical thresholding devices, Adv. Opt. Mater. 6 (2018) 1701166.

[58] Z. Sun, A. Martinez, F. Wang, Optical modulators with 2D layered materials, Nat. Photonics 10 (2016) 227.

[59] D.H. Kang, M.S. Kim, J. Shim, J. Jeon, H.Y. Park, W.S. Jung, H.Y. Yu, C.H. Pang, S. Lee, J.H. Park, High-performance transition metal dichalcogenide photodetectors enhanced by self-assembled monolayer doping, Adv. Funct. Mater. 25 (2015) 4219–4227.

[60] J. Honig, J. Spałek, Electronic Properties of NiS2-x Se x Single Crystals: From Magnetic Mott − Hubbard Insulators to Normal Metals, Chem. Mater. 10 (1998) 2910–2929.

[61] G. Krill, M. Lapierre, C. Robert, F. Gautier, G. Czjzek, J. Fink, H. Schmidt, Electronic and magnetic properties of the pyrite-structure compound NiS2: influence of vacancies and copper impurities, J. Phys. C: Solid State Phys. 9 (1976) 761.
[62] T. Anand, K. Rajes, M. Zaidan, Electro synthesized NiS2 Thin Films and Their Optical and Semiconductor Studies, Rep. Electrochem. 3 (2013) 25–29.
[63] S. Wang, H. Yu, H. Zhang, A. Wang, M. Zhao, Y. Chen, L. Mei, J. Wang, Broadband few-layer MoS2 saturable absorbers, Adv. Mater. 26 (2014) 3538–3544.
[64] Y. Xu, M.A. Schoonen, The absolute energy positions of conduction and valence bands of selected semiconducting minerals, Am. Mineral. 85 (2000) 543–556.
[65] S. Li, Y. Yin, Q. Ouyang, G. Ran, Y. Chen, E. Lewis, G. Farrell, M. Tokurakawa, S.W. Harun, P. Wang, Nanosecond passively Q-switched fibre laser using a NiS 2 based saturable absorber, Opt. Express 27 (2019) 19843–19851.
[66] C. De las Heras, F. Agulló-Rueda, Raman spectroscopy of NiSe2 and NiS2-xSex ($0 < x < 2$) thin films, J. Phys.: Condens. Matter 12 (2000) 5317.
[67] J. Nicholson, R. Windeler, D. DiGiovanni, Optically driven deposition of single-walled carbon-nanotube saturable absorbers on optical fiber end-faces, Opt. Express 15 (2007) 9176–9183.
[68] X. Liu, D. Han, Z. Sun, C. Zeng, H. Lu, D. Mao, Y. Cui, F. Wang, Versatile multi-wavelength ultrafast fiber laser mode-locked by carbon nanotubes, Sci. Rep. 3 (2013) 2718.
[69] Y. Cui, F. Lu, X. Liu, Nonlinear saturable and polarization-induced absorption of rhenium disulfide, Sci. Rep. 7 (2017) 40080.
[70] J. Boguslawski, G. Sobon, R. Zybala, J. Sotor, Dissipative soliton generation in Er-doped fiber laser mode-locked by Sb 2 Te 3 topological insulator, Opt. Lett. 40 (2015) 2786–2789.
[71] L. Zhao, D. Tang, H. Zhang, X. Wu, Q. Bao, K.P. Loh, Dissipative soliton operation of an ytterbium-doped fiber laser mode locked with atomic multilayer graphene, Opt. Lett. 35 (2010) 3622–3624.
[72] X. Li, Y. Wang, Y. Wang, W. Zhao, X. Yu, Z. Sun, X. Cheng, X. Yu, Y. Zhang, Q.J. Wang, Nonlinear absorption of SWNT film and its effects to the operation state of pulsed fiber laser, Opt. Express 22 (2014) 17227–17235.
[73] H. Kotb, M. Abdelalim, H. Anis, Generalized analytical model for dissipative soliton in all-normal-dispersion mode-locked fiber laser, IEEE J. Sel. Top. Quantum Electron. 22 (2015) 25–33.
[74] J. Buckley, F. Wise, F. Ilday, T. Sosnowski, Femtosecond fiber lasers with pulse energies above 10? nJ, Opt. Lett. 30 (2005) 1888–1890.
[75] G.P. Agrawal, Nonlinear fiber optics, Nonlinear Science at the Dawn of the 21st Century, Springer, 2000, pp. 195–211.
[76] W. Li, B. Chen, C. Meng, W. Fang, Y. Xiao, X. Li, Z. Hu, Y. Xu, L. Tong, H. Wang, Ultrafast all-optical graphene modulator, Nano Lett. 14 (2014) 955–959.
[77] Y. Cui, F. Lu, X. Liu, MoS 2-clad microfibre laser delivering conventional, dispersion-managed and dissipative solitons, Sci. Rep. 6 (2016) 1–8.
[78] G. Yang, Y.-G. Liu, Z. Wang, J. Lou, Z. Wang, Z. Liu, Broadband wavelength tunable mode-locked thulium-doped fiber laser operating in the 2 μm region by using a graphene saturable absorber on microfiber, Laser Phys. Lett. 13 (2016) 065105.
[79] J. Liu, Y. Chen, Y. Li, H. Zhang, S. Zheng, S. Xu, Switchable dual-wavelength Q-switched fiber laser using multilayer black phosphorus as a saturable absorber, Photonics Res. 6 (2018) 198–203.
[80] G. Wang, G. Chen, W. Li, W. Zhang, C. Zeng, W. Zhao, Indium selenide as a saturable absorber for a wavelength-switchable vector-soliton fiber laser, Opt. Mater. Express 9 (2019) 449–456.
[81] Y. Zhao, P. Guo, X. Li, Z. Jin, Ultrafast photonics application of graphdiyne in optical communication region, Carbon 149 (2019) 336–341.
[82] K. Zhang, M. Feng, Y. Ren, F. Liu, X. Chen, J. Yang, X.-Q. Yan, F. Song, J. Tian, Q-switched and mode-locked Er-doped fiber laser using PtSe 2 as a saturable absorber, Photonics Res. 6 (2018) 893–899.
[83] M. Zhang, R.C. Howe, R.I. Woodward, E.J. Kelleher, F. Torrisi, G. Hu, S.V. Popov, J.R. Taylor, T. Hasan, Solution processed MoS 2-PVA composite for sub-bandgap mode-locking of a wideband tunable ultrafast Er: fiber laser, Nano Res. 8 (2015) 1522–1534.